Arab J Geosci (2017) 10: 235
DOI 10.1007/s12517-017-3029-6

ORIGINAL PAPER

Coupling of field investigations and remote sensing data for karst hazards in Egypt: case study around the Sohag City

Ahmed M. Youssef[1,2] · **Abdel-Hamid El-Shater**[1] · **Mohamed H. El-Khashab**[1] · **Bosy A. El-Haddad**[1]

Received: 15 June 2016 / Accepted: 14 May 2017 / Published online: 30 May 2017

Abstract Karst rocks cover a wide area of Egypt. These rocks include soluble sediments such as carbonate rock formations, evaporites, and sabkha deposits that are characterized by karstification features. Karst features could affect many current and developing projects (urban areas and infrastructure). The areas covered by the rocks susceptible to karstification need detailed studies to examine the presence of karst features and/or sinkholes. The current work provides a detailed evaluation of the karst and/or sinkhole hazards around the city of Sohag, Egypt. This research is rarely done in Egypt, using field investigation and remote sensing application to determine the main karstic rock formations and the distribution of the most problematic sinkhole areas. In this work, different types of the subsidence mechanisms were investigated. Our results indicated that field investigations help in finding different features related to karstification including small-scale versus large-scale features and empty caves versus filled caves. In addition, remote sensing techniques succeeded in predicting and locating the sinkhole areas, and those determinations were verified in the field. Finally, fundamental considerations are discussed to better evaluate and manage the hazard of karst and/or sinkholes.

✉ Ahmed M. Youssef
amyoussef70@yahoo.com

Bosy A. El-Haddad
bosy_abdelaziz@hotmail.com

[1] Geology Department, Faculty of Science, Sohag University, Sohag, Egypt

[2] Geological Hazards Department, Applied Geology Sector, Saudi Geological Survey, P.O. Box 54141, Jeddah 21514, Kingdom of Saudi Arabia

Keywords Karst · Geohazards · Detection · Investigation · Egypt

Introduction

Karst is a geomorphologic feature that is formed in soluble rocks and/or sediments by widening existing fractures or cavities through the dissolution activities (Youssef et al. 2016). Amin and Bankher (1997) indicated that the dissolution of karst units forms sinkholes that represent subsidence hazards in Saudi Arabia. The dissolution process of the subsurface materials causes collapse of the overburden materials resulting in the formation of sinkhole depressions (White 1988). Ford and Williams (2007) mentioned that the surface and subsurface rock dissolution mechanism largely overrules the mechanical erosion mechanism, leading to a distinctive morphology and hydrology in karst areas. Karst systems are distinct from non-karst systems because of the processes of karst dissolution and the presence of a well-developed and open subsurface (Gunn 2004). White (2002) indicated that karst processes, along underground pathways, may give rise to the formation of three-dimensional systems of conduits, sometimes forming huge, long, and extremely complex caves. White (2007) mentioned that cave exploration gives valuable information in studying karst aquifers. The formation of caves, collapsed caves, and sinkholes due to the karst development make the karst features are very distinctive. A sinkhole inventory map is one of the main steps in sinkhole susceptibility analysis, hazard evaluation, and risk management. Karst cavities represent major problems in many areas all over the world such as in The Apulia region of southern Italy (Parise 2006); in China (Gao et al. 2013); in the Bambuí Group, Brazil (De Carvalho et al. 2014); in NW-Morocco (Theilen-Wilige et al. 2014); and in Saudi Arabia (Youssef

et al. 2016). The presence of these problems cause damage to human structures (Waltham et al. 2005), human life loss (Gao et al. 2013; Gutiérrez et al. 2010), water leakage in reservoirs (Gutiérrez et al. 2014a), instability problems (Song et al. 2012), and flooding and water table rise (Crawford 1984). Different types of distinguishing surface features can be used in recognizing the karst landforms using field and remote sensing data. Features could be recognized using remote sensing data such as Landsat enhanced thematic mapper plus (ETM^+) and professional Google Earth including ring, circular, and oval features and depressions, sinkhole clusters, and aggregate accumulations (Youssef 2008a; Youssef et al. 2012, 2016). Other karst features could be distinguished in field investigation such as sagging of the roof beds, collapse breccia, and the solution deposits in the fractures.

In Egypt, karst rocks cover a large area including wide areas along the eastern and western limestone plateaus (Halliday 2003) which overlook the Nile valley from Luxor to Cairo and evaporite rocks and sabkha areas that are located along the Red Sea coast. The destruction and damage related to karst and sinkhole activities have substantially increased in the last decade in Egypt due to the rapid increase in development activities that extend to cover areas that are prone to karst hazards. The insufficient understanding of karst in limestone and evaporite bedrock can cause serious construction problems and losses in properties and lives. There are several studies documenting karst landforms that are found in Egypt, especially sinkholes and caves. Hume (1925) recorded the presence of some caves in Wadi Um Dud east of the Tahta City and depicted the location of "Great Cavern" and unnamed caves in Wadi Qasab and Wadi Abu Nafukh eastern south of Sohag City. El-Sayed (1995) described small karstic features such as sinkholes and caves with dripstone up to 0.8-m long in the Farafra area in the Wadi al-Obayyid. El-Ramly (1997) studied karstic pollution and subsidence problems of the Mokattam area. The Mokattam karst, which is formed on the dissected limestone plateau on the eastern fringe of metropolitan Cairo, represents a famous example in Egypt. Khalil and Hassan (1997) and Khalil et al. (2002) mentioned that the karstic waters in the Western Desert characteristically arise from fissures in the underlying Nubian sandstone and with lesser quantities flow in fractured limestone rocks. Halliday (2000, 2003) indicated that several significant karstic features were located in the north southern Galala plateau such as St. Anthony's cave. Halliday (2003) indicated that the most beautiful and important caves in Egypt is that of Wadi Sannur which is considered as a potential World Heritage Site. Ruggieri (2001) reported the occurrence of small caves along the road from Edfu to Dush in the Kharga oasis and in Wadi Karnak. Brook et al. (2002) described one of the most important caves in this western plateau, which is known as Djara Cave (40 m long). It is located between Assiut and Farafra Oasis and resulted from the dissolution of carbonates. Pielsticker (2002) explained the occurrence of the Egyptian Alabaster near the road of Farafra-Baharya oasis by the unroofing of a large cave. Wanas et al. (2009) indicated that some karst features were located in the area between El-Baharia and El-Farafra oases in the Western Desert. Abdeltawab (2013) mentioned that the area between El-Minia and Maghagha also shows some karst features.

Karst and sinkhole evaluation in Egypt represent a little explored topic. Therefore, the current study represents a new work that could help in understanding and evaluating the karst phenomena in Egypt, using field investigation and remote sensing applications. The current research provides an overview of the karst problem around Sohag City, Egypt (Fig. 1). It determines the essential karst formations and the distribution of the most problematic karst areas (sinkhole and cave areas). These were illustrated through many karst feature types covering the study area with different subsidence mechanisms.

Study area characteristics

Sohag governorate lies in the middle part of the Nile Valley which is situated south of Cairo by about 460 km between the latitudes 26° 6′ 54″ to 27° 9′ 26″ N and longitudes 31° 13′ 18″ to 32° 36′ 50″ E (Fig. 1). The Sohag City is bounded from east and west by the limestone plateau in which there are many wadis that dissect the plateau, and has a main direction NE-SW; following these plateau inwards, there are low desert land areas and agricultural areas surrounding the River Nile. The limestone plateaus, in Sohag District, border the low land desert from west and east and represent part of the major Eocene Limestone plateau of the Eastern and Western Deserts of Egypt. It rises about 200 to 300 m above sea level and generally decreases toward the north. Structurally, the limestone plateaus surrounding the Sohag City are characterized by many joints with different directions NW-SE (main direction), NE-SW, and E-W. These joints have an essential effect in the karstification processes due to the movement of water through them. Sohag area belongs to the arid belt of Egypt, which is characterized by dry climate. The rainfall in the area is variable from time to time during the year with a yearly average ranging between nill in summer to 17 mm in winter. The rainfall in the Sohag area is very irregular and sometimes it happens suddenly with high rate causing flash floods (Kareim 2001). The average temperature in the area is about 23.2°. The highest temperature is recorded in August while the minimum is recorded in January with an average between 14 and 30.8 °C.

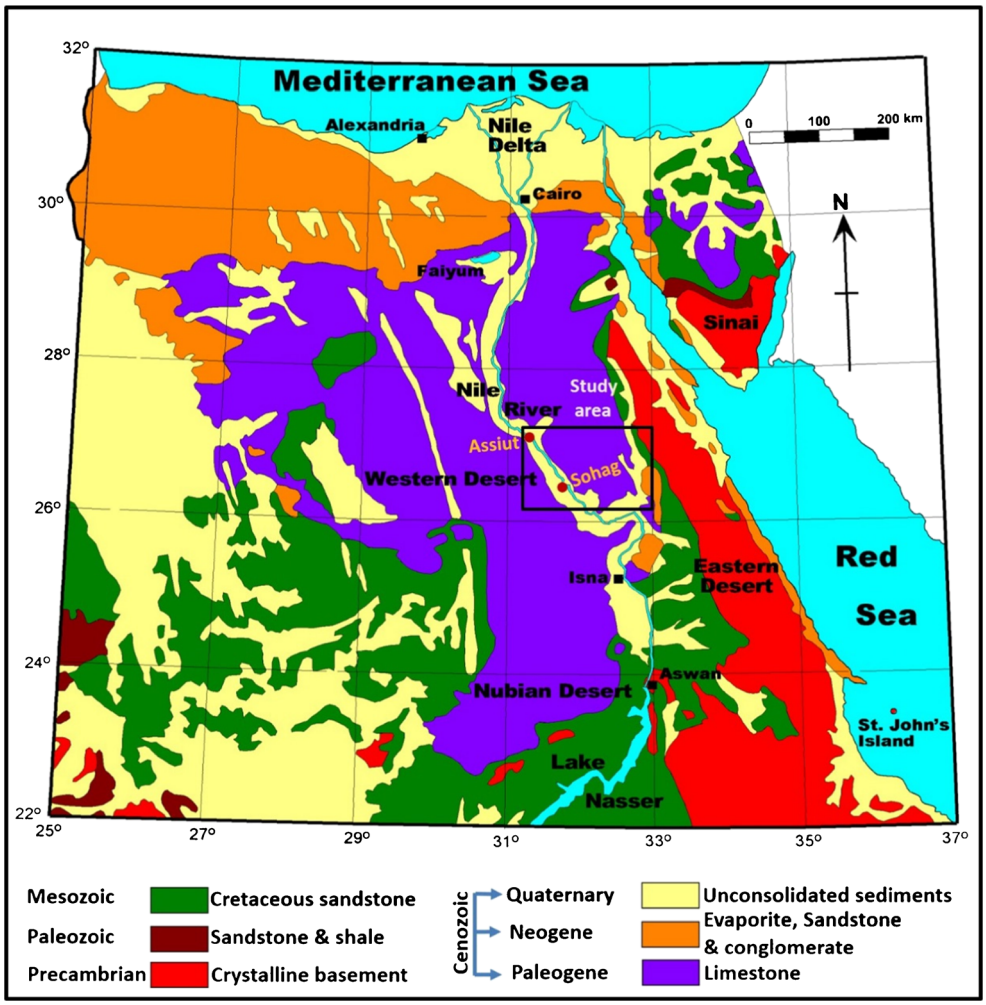

Fig. 1 Generalized geological map of Egypt (http://www.eeescience.utoledo.edu/Faculty/Harrell/Egypt). *Black box* represents the study area

Distribution of sinkhole-prone areas in Egypt

Egypt, located on the northeastern part of the African Continent, comprises four geological zones with different lithological, structural, and geomorphological features (Fig. 1): (1) Zone (1): Precambrian rocks: they are called the Nubian Shield, situated on the Eastern part of Egypt, and mainly consists of igneous and metamorphic rocks. Karst-related features are rare or absent in this zone. (2) Zone (2): Paleozoic rocks: they consist of sandstone and shale. They are exposed in some small areas in Egypt especially the south western corner and southern Sinai. (3) Zone (3): Mesozoic rocks: they consist of sandstone and some carbonates of Cretaceous age. They are exposed in some areas in Egypt especially the southern part and middle section of Sinai. (4) Zone (4): Cenozoic rocks: they consist mainly of three groups, namely, (a) limestone rocks that are related to Paleogene which covered the middle part of eastern and western plateau, which sometimes is covered by Quaternary deposits and the middle of Sinai; (b) Neogene evaporite, sandstone, and conglomerates covering a narrow coastal area of the Red Sea, east of the Nubian Shield, and the north western area of Egypt and the eastern side of Suez Gulf; and (c) undifferentiated sediments that cover west, north, and along the Red Sea cost and Nile valley of Egypt.

Methodology

The main investigation methods are presented in the current study, including field investigation and remote sensing application. Field investigation was carried out to conduct a detail study of different features of karst processes and verification of the remote sensing results. Remote sensing data used in the current study including Landsat 7 ETM^+ and Google Earth images. Google Earth images have a high resolution (<1 m pixel size), which provides good opportunities to detect and map sinkholes and karst features. In the current study, two methods of detections were applied. First according to visual interpretation of ETM^+ and high-resolution satellite images (Google Earth images). The second method by using enhanced processing of the ETM^+ images to automate recognition of susceptible sinkhole and karst areas. The material used

in this analysis consists of Landsat 7 ETM$^+$ imagery Path175, Row 42, acquired on 2000. The image is cloud free and geometrically corrected to a UTM Zone 36 north and WGS84 datum. Landsat ETM$^+$ is multi-spectral remote sensing data that have eight bands of the electromagnetic spectrum. The image processing has been done using the Environment for Visualizing Images (ENVI 5) software. The ETM$^+$ bands 1, 2, 3, 4, 5, and 7 were stake together to build one image with 30-m resolution. The produced image was fused with band 8 to produce a final image of the study area with 15-m spatial resolution. Different image processing techniques were employed including principle component analysis (PCA), minimum noise fraction (MNF), and hue saturation value (HSV).

Results and discussion

Karstification-susceptible units in the area around the Sohag City

Despite the arid climate of Egypt (the annual rainfall precipitation is less than 100 mm), many caves, sinkholes, and karstification features were detected recently, notably in El-Minia, Sohag, Assiut, and other areas. Most of the recent documented caves, sinkholes, and other karstification features are associated with human activities that may favor or trigger dissolution and/or subsidence processes. Limestone rocks in the area around Sohag are classified into two formations: the Thebes Formation and the Drunka Formation.

Thebes Formation was introduced by Said (1960) to describe the laminated and massive cherty limestone. This formation represents the lower part of the Eocene limestone of the Nile Valley that conformably overlies the Esna shale. It occupies the foot of the limestone scarp at the area around the Sohag City with a thickness of 150 m, and constitutes most of the eastern limestone scarp, and extends from Wadi Qasab-Wadi Abu Nafoukh in the south to Awlad El Shekh in the north. In the area, west and southwest of Sohag, the Thebes Formation (up to 110 m thick) is composed of fine grained, massive to laminated limestone with flint bands. The banded flinty limestone succession is easily separated from the overlying "Drunka Formation." No karst features, "sinkholes, or caves" were detected of the Thebes Formation.

The term Drunka Formation was first introduced by El Naggar (1970) to describe the stratigraphic succession overlying the Luxor Formation and is exposed with a thickness of more than 200 m in the type locality at Gabal Drunka, southwest of Assiut. Mostafa (1979) stated that Drunka Formation covers ~90% of the area east and northeast of Sohag City. Most of the scarps in the study area are composed of Drunka Formation, which has a wide extension outside this area. In the study area, the Drunka Formation overlies the Thebes Formation. The Thebes Formation is easily differentiated from Drunka Formation by its white color, massive bedding, and the abundance of large silicified carbonate concretions. Field studies indicated that the lower part of the Drunka Formation (about 30 m) forms a transition zone between the Thebes and the lower Drunka Formation, which is characterized by the presence of silicified concretions (up to 1.2 m in diameter). The upper part of the Drunka succession (up to 100-m thickness) is composed of grayish white, massive to bedded bioturbated limestone. The abundance of Echinoderms, Molluscs, calcareous algae, large Foraminefra, as well as the widely distributed bioturbation all may indicate that the sediments of the Drunka Formation were deposited under near shore condition (Laporte 1971; Wilson 1975; Mostafa 1979). The Drunka Formation is characterized by the presence of karst features including caves of different sizes as well as depressions.

Karst types and mechanisms

The current work follows the genetic sinkhole classification introduced by Gutiérrez et al. (2008, 2014b). This genetic classification used two main sinkhole categories called solution and subsidence sinkholes. Solution sinkholes represent shallow enclosed depressions, due to the differential erosion of the exposed karst rock surface. Development of this type of sinkhole is guided by discontinuities, does not involve the settlement of the land surface, and consequently do not produce a ground instability hazard. Subsidence sinkholes are related to subsurface dissolution and controlled by downward gravitational movement of the undermined overlying sediments. The subsidence sinkholes are responsible of surface deformation, damages, and/or internal erosion of the sediments and/or rocks. Gutiérrez et al. (2010) indicated that the genetic sinkhole classification is applicable to karstic rocks (carbonate and evaporate rocks). Two terms were used to describe subsidence sinkholes. The first term characterizes the subsidence materials into cover (represents loose deposits), bedrock (refers to karst rocks), and cap rock (describes non-karst rocks). The second term describes the subsidence mechanism including collapse (refers to brittle deformation of soil or rock materials), suffosion (indicates downward migration of loose cover deposits through conduits and progressive settling), and sagging (means downward bending of ductile sediments and/or rocks). Complex sinkholes could be formed which characterized by the presence of different material types and many subsidence mechanisms. In the current work, different types of sinkholes were recognized in the study area as shown in (Fig. 2).

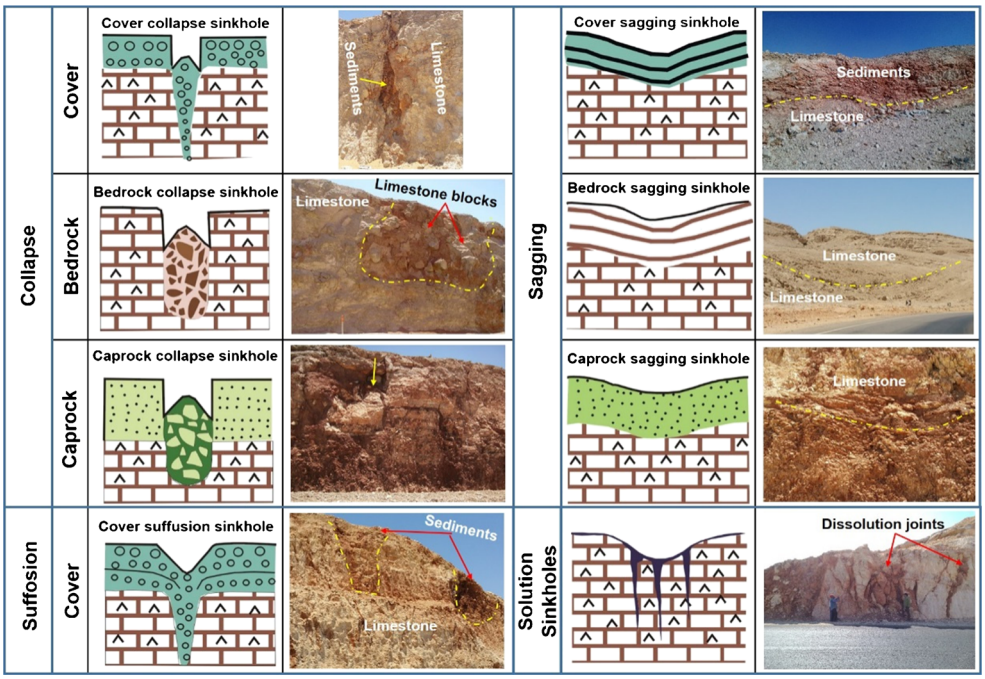

Fig. 2 Sinkholes classification in the study area (the generic classification of sinkholes is according to Gutiérrez et al. (2008, 2014b)

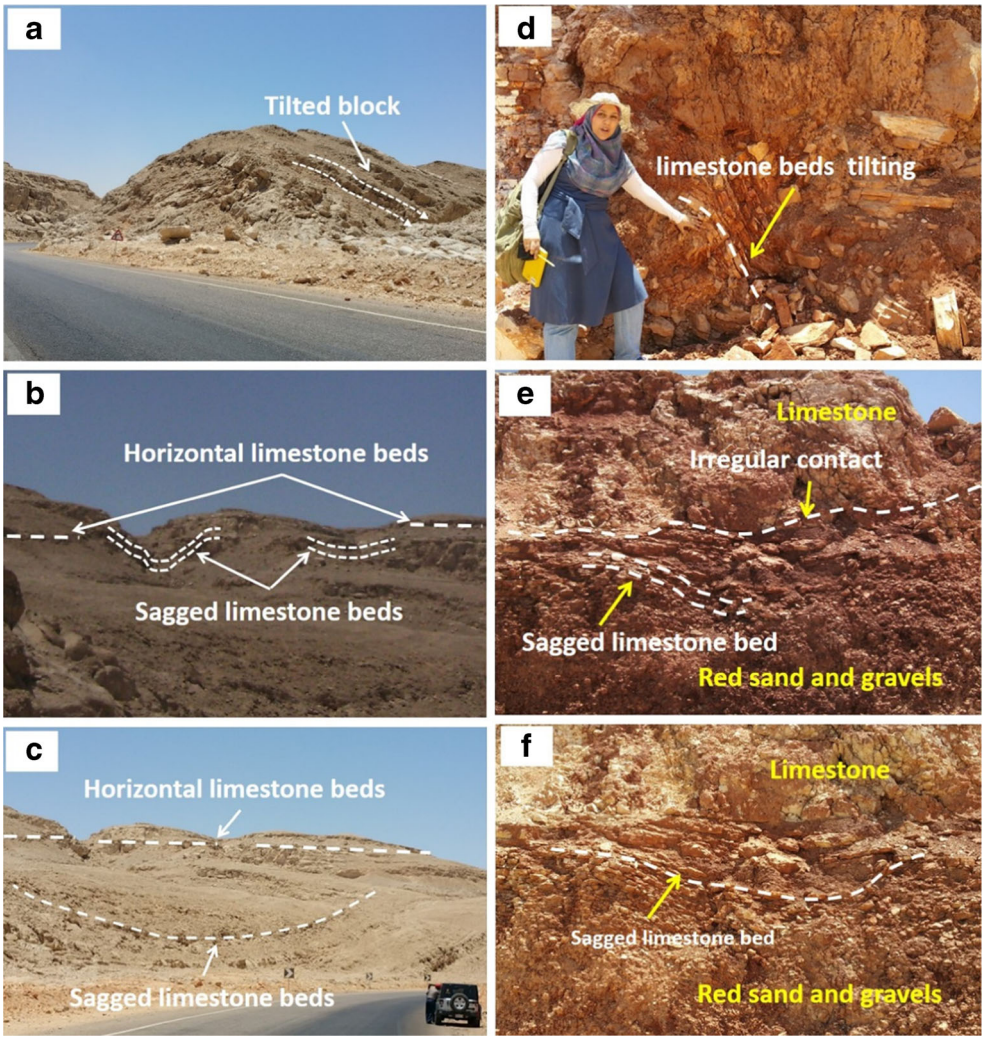

Fig. 3 **a**–**c** Large-scale karstification features and **d**–**f** small-scale karstification features inside the filling caves materials

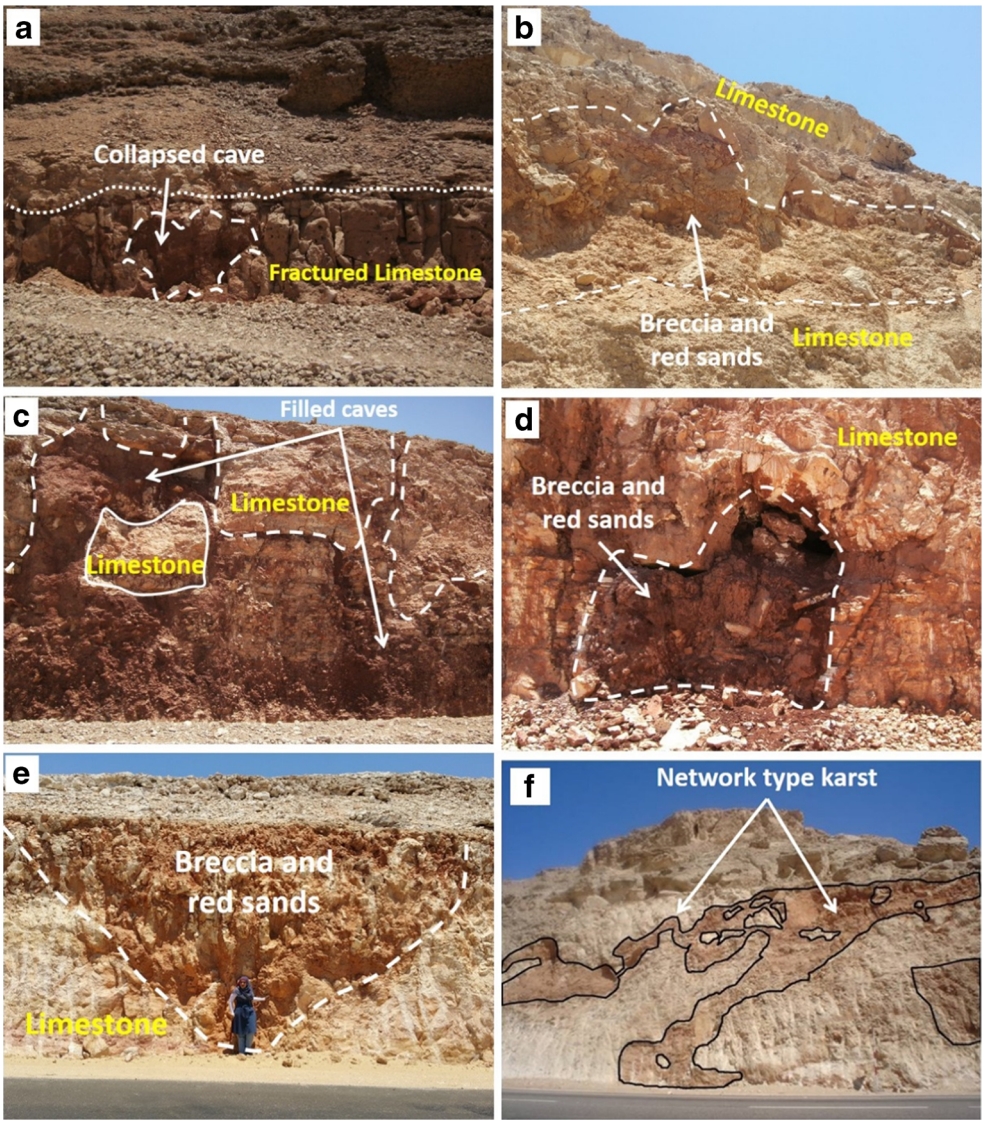

Fig. 4 Several collapsed caves showing different karst features. **a**–**e** show buried sinkhole filled with weakly cemented red sand and coarse brecciated materials (sand and fine materials with big boulders of limestone fragments). These limestone blocks resisted the dissolution and represent the caves remnants of network type karst

Field identification and characterization of karst in the study area

Field investigations were conducted in the area around Sohag City including the Sohag-Assiut asphaltic road and Sohag-Red Sea road. Several karst features were detected and investigated in detail in the Drunka limestone Formation. The Drunka limestone Formation in the study area is characterized by bioturbation, joints, fissures, and fractures which facilitate the process of dissolution of limestone and trigger the formation of caves, sinkholes, and collapsed caves. Several features from this kind were detected along these asphaltic roads.

Large- versus small-scale features

The dissolution of the limestone in the area around the Sohag City is very common. The field investigations which were conducted in the area east and west of Sohag led to detection of several karst features. The karst features are well represented as subsidence, tilting, and sagging of the limestone beds (Fig. 3a–c). Small features were also detected inside the filling materials of the caves. These features were formed during the formation of these karst features including tilting of the laminated limestone beds (Fig. 3d, e) and sagging of the beds due to the loading of the massive limestone located at the top of the filling caves (Fig. 3f).

Filled caves versus empty caves

Karst features exemplified in the study area by the well-known filled sinkhole and/or cavities (along the rock cuts and the wadis that cut the limestone plateau). Large numbers of these cavities can be seen along the road cut of the western desert highway (Cairo-Aswan) and the eastern desert highway (Sohag-Red Sea highway). Karst features in this area are of different types: (a) pockets, (b) networks parallel to the strata

or joints, indicating the preferential circulation of water along discontinuities representing bedding planes, and (c) empty voids and cavities. Detailed analysis of the caves infilling materials varies from place to place, and in general, four facies of deposition were detected (Fig. 4): (1) a coarse basal breccia is composed of material derived from the country rock, blocks of white chalk, limestone, and some chert with diameters ranging from few centimeters to 1 m (Fig. 4b, d, e), and the large boulders of the limestone represent the remnants of the caves before the collapse (Fig. 4c); (2) locally red sands with muddy matrix (Fig. 3d–f); (3) coarsely crystalline gray calcite, occasionally forming masses up to few meters and more than 5-m wide and long (Fig. 5b, c), and calcite in the cave varies from microcrystalline varieties to layers of huge crystals up to 15 cm; and (4) deformed and fragmented limestone. In this facies, the original bedding of limestone can be seen in spite of the deformation and fragmentation (Fig. 3d). In most of the caves (empty and filled caves), the roof materials are massive limestone (Figs. 4b–d and 5a–e).

As an example of the biggest caves on this road is at latitude 26° 52′ 42.2″ N and longitude 32° 14′ 04.1″ E, its opening reaches 3.1 m and its height reaches 9 m (Fig. 5a). Field investigations indicated that there is a main joint that has the major impact on the cave area. It represents the main pathway of the water toward the cave. The joint bearing is N76°E (Fig. 5d). Some stalactites and stalagmites are found in the cave which range from soda straw forms to large tapered types. Some of them have secondary coatings of different thickness. Others are glassy and they appear as a monocrystalline (Fig. 5b, c). Other empty caves were recognized in the area west of Sohag City. Series of empty caves were recognized as extending to 21 m in width and up to 2 m in height of the opening. These caves extend within the limestone

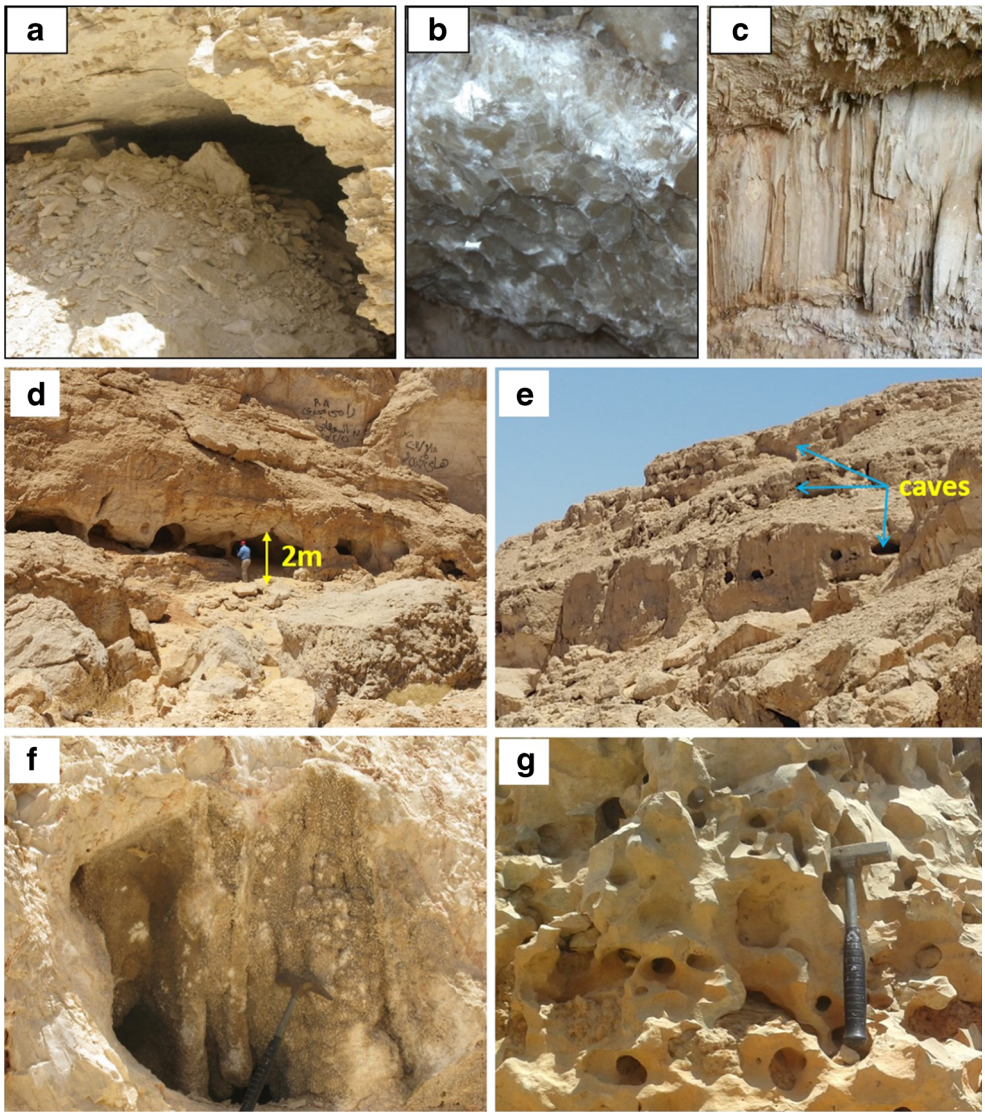

Fig. 5 **a** One of the largest caves along Sohag-Red Sea highway (an entrance opening of 8-m wide and 3-m height). **b** Calcite crystals on the roof of the cave. **c** Many stalactite and stalagmite structures inside the cave. **d**, **e** show an example of local cavities more than 10 m in size, which were found along western desert Cairo-Aswan highway. **f**, **g** show probably cavernous weathering of limestone in the study area

plateau for several meters (Fig. 5d, e). Other features such as bioturbation and small caves were detected (Fig. 5f, g).

In the study area, it is essential to mention that the nature of the upper part of the limestone plateau (Drunka Formation) is characterized by many joints, fractures, and faults which make this rock formation favorable to form karst phenomena (Fig. 6). These joints and fractures could be considered as the pathways for the infiltration water which play a major role in limestone dissolution and cave formations. Grosch et al. (1987) indicated that most of karst features are controlled by joint systems. These karst features were developed during the past pluvial periods.

Application of remote sensing in karst detection

Land use planning in karst terrains mostly relies on detailed mapping of sinkholes and karst features. Sinkholes can be recognized from topographic maps as closed depression features (Alexander et al. 2013; Youssef et al. 2016). However, there are some problems using topographic maps for detecting sinkholes such as (1) most of these topographic maps are old and new sinkholes may have developed recently, (2) not all closed depressions in the topographic maps are sinkholes, and (3) some small sinkholes and karst features cannot be recognized on topographic maps due to scale. In addition to that essential and important information on sinkhole distribution and evolution can be extracted from aerial photographs (Carbonel et al. 2015; Gutiérrez et al. 2011). Unfortunately, aerial photographs in many areas are not available. However, with the development of remote sensing images such as Landsat Enhanced Thematic Mapper Plus (ETM^+), surface features related to karstification and sinkholes could be easily detected and mapped (Newton 1976; Youssef et al. 2012, 2016). High-resolution and accuracy of remote sensing images provide good opportunities to detect and map sinkholes and karst features. The remote sensing detection of sinkholes and karst features are due to highly subdued geomorphic expression (Youssef et al. 2012, 2016). Dinger et al. (2007) used high-resolution images (1 m) to detect circular shapes as indication of sinkholes. Guimarães et al. (2005) used Advanced Spaceborne Thermal Emission and Reflection Radiometer (ASTER) data to detect karst depressions depending on a combination filtering and digital classification of spectral images techniques. Siart et al. (2009) used a combination of digital elevation data, high-resolution images, and GIS to detect and map karst features. In the current study, two methods of detections were applied. First, according to visual interpretation of ETM^+

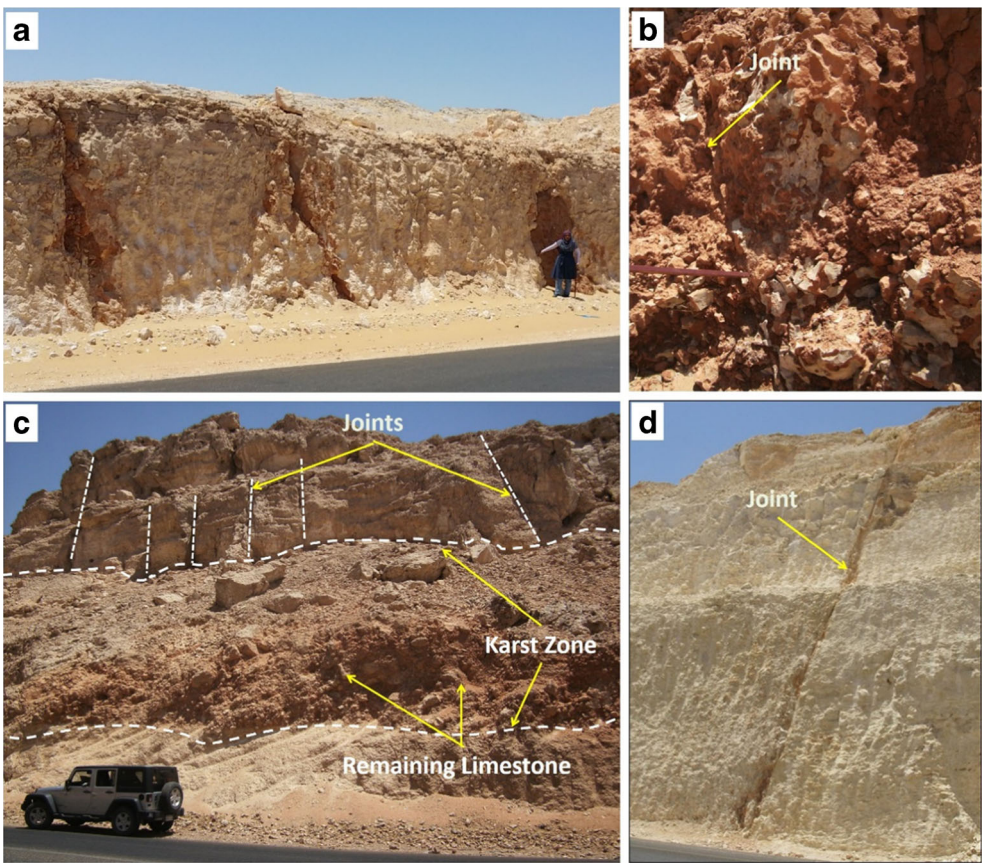

Fig. 6 **a**–**d** Photograph showing different joints in Drunka Formation that activate the karst formation

and high-resolution satellite images (Google Earth images). The second method by using enhanced processing of the ETM$^+$ images to automate recognition of susceptible sinkhole and karst areas.

Results of visual interpretation

The reference map of karst and sinkhole features was built from the visual interpretation of ETM$^+$ (15 m), professional Google Earth images (<1 m), and detailed field validation. These images were used to detect different karst and sinkhole features such as circular and oval depression features and ring structures. In the current study, circular and oval sinkhole features were mapped. They appeared as subtle peripheral ridges and an internal depression (few meters deep) with a diameter or main axial length ranging from a few hundred meters to some kilometers (Fig. 7). Accordingly, these mapped sinkholes and karst features were verified with the field investigation.

Results of ETM$^+$ analysis

In the current study, sinkhole and karst feature mapping have four steps, building ETM$^+$ image composite with 30-m resolution, using the/a fused method to prepare ETM$^+$ with 15-m resolution, apply different enhanced techniques to map susceptible sinkhole and karst areas, and field checking.

In the first step, the layer stacking was performed for bands 1, 2, 3, 4, 5, and 7 to produce a composite image using Erdas Imagine (v. 9.2).

In the second step, the layer stack mosaic (30-m spatial resolution) was sharpened using panchromatic band (band 8) (15-m special resolution) to produce a composite of ETM$^+$ image with a spatial resolution of 15 m. Image subsetting was applied to produce image for the study area as shown in Fig. 8a.

In the third step, the latter composite image (15-m resolution) was used to map the most susceptible areas for sinkholes and karst areas. In this method, it was assumed that most of the caves are filled with red sediments. The mapping technique was done by applying three enhanced techniques including principle component analysis (PCA), minimum noise fraction (MNF), and hue saturation value (HSV). (a) The principle component analysis (PCA) depends on the analysis of principal components which applied on the original bands of the multispectral image to produce an equal number of components (Crosta and Moore 1989). PCA is a multivariate statistical technique which selects uncorrelated linear combinations of variables with a small variance (Singh and

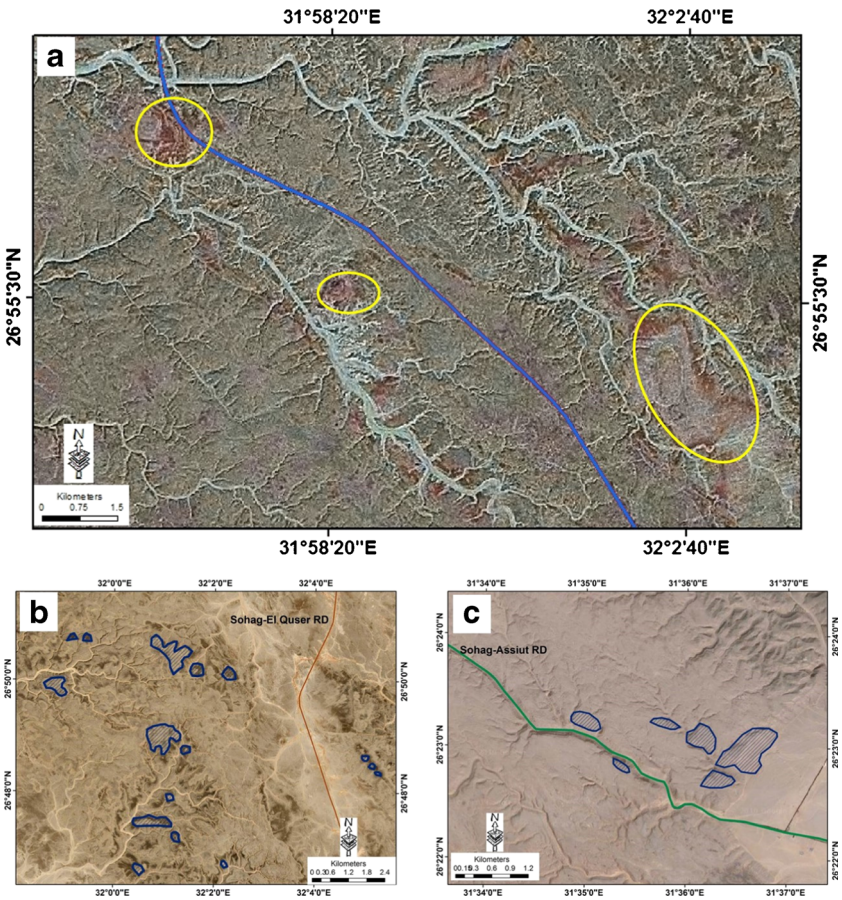

Fig. 7 Reference maps from the visual interpretation: **a** Distribution of the dissolution depressions were detected from ETM$^+$ 15-m resolution (yellow ovals). **b**, **c** Google Earth images show several depression with different sizes and shapes (oval and circular) at the top of the limestone plateau; around the Sohag-Red Sea highway (**b**) and around Sohag-Assiut highway (**c**)

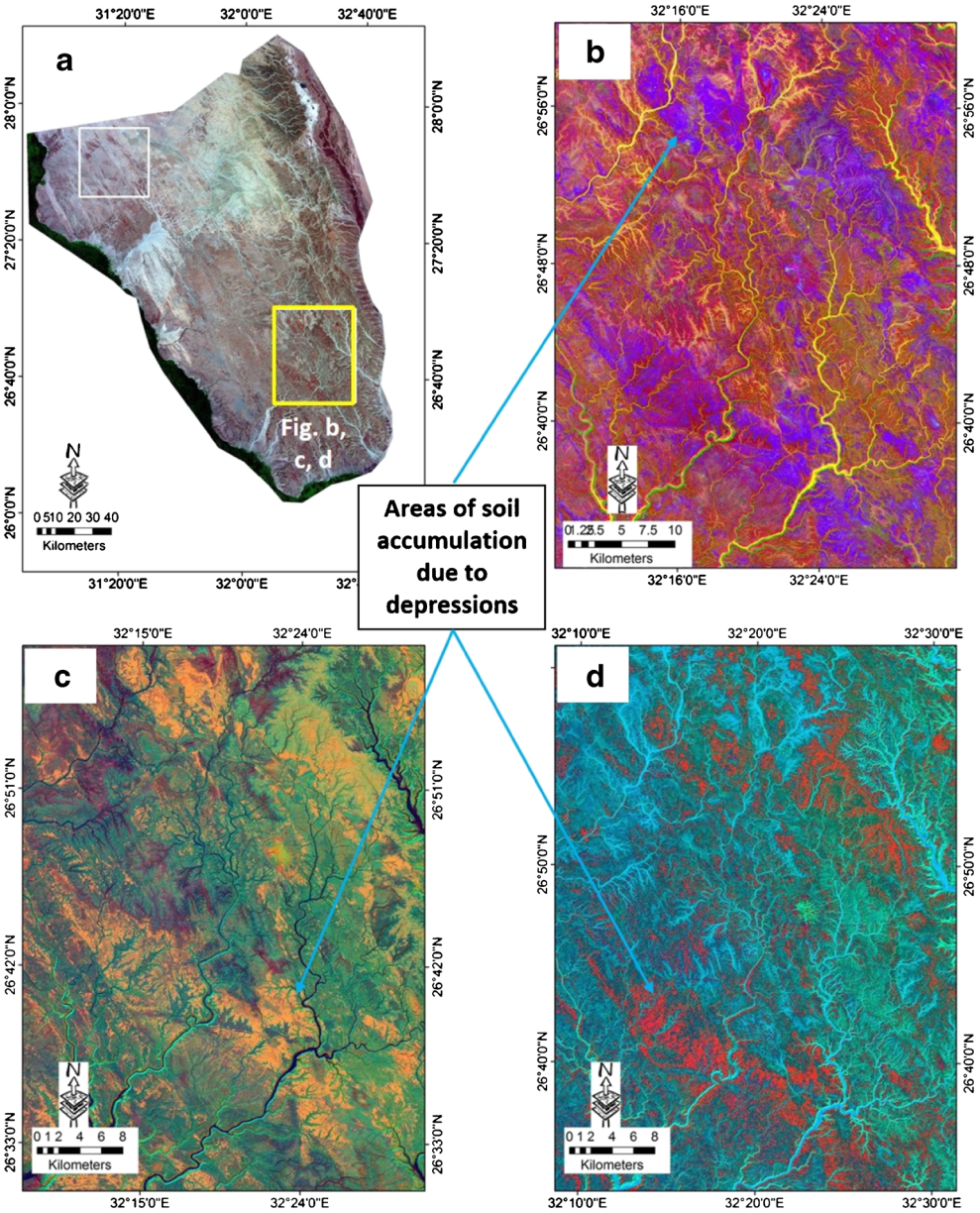

Fig. 8 **a** ETM$^+$ 15-m resolution (RGB 742), **b** PCA 123, **c** MNF 512, and **d** HSV

Harrison 1985). The main aim of PCA is to overcome redundancy in multispectral data. PCA is widely used for mapping of alteration zones, aggregate materials, and Pliocene clay (Tangestani and Moore 2002; Ranjbar and Honarmand 2004; Youssef 2008a, b). In the current study, PCA was applied on bands 1, 2, 3, 4, 5, and 7 of the ETM$^+$ image. The PC transformation result indicates that PCA bands 1, 2, 3 in RGB, respectively, are successful in detecting and distinguishing the filled sinkhole areas from the surrounding materials (Fig. 8b). (b) The minimum noise fraction (MNF) method is a common method applied to determine the inherent dimensionality, to segregate noise, and to reduce the computational of the image data for further processing (Boardman and Kruse 1994). Green et al. (1988) indicated that the MNF transform is characterized by two types of principal component transformations. The first transformation is based on estimation of noise covariance matrix. It depends on band-to-band correlations. The second step is called standard principal component transformation of the noise whitened data. For further spectral processing, the inherent dimensionality of the data is identified based on examination of the eigenvalues and the associated images. The data is divided into two groups. The first group is associated with large eigenvalues and coherent eigen images, and a complimentary part with near unity eigenvalues and noise dominated images. However, the noise could be separated from the data and improving the spectral processing results by using the coherent portions. The result of the current study indicated that the first three bands have large eigenvalues. They are the most important bands to represent the spectral information. Figure (8c) shows the combination of

MNF 5, 1, 2 in RGB, respectively. They are clearly distinguished from the areas of filled sinkholes from the surrounding materials. (c) Hue saturation value (HSV) represents a color model. It describes colors (hue or tint) in terms of their shade (saturation or amount of gray) and their brightness (value or luminance). Firstly, the original image transforms into the HSV color space. The input file has at least three bands or a color display open to use this function. The stretch is applied in the color display to the input data. In the current study, the HSV was applied on original ETM^{+} image bands 742 in RGB. The results indicated that the HSV method is clearly marking out the areas of filled sinkholes from the surrounding deposits (Fig. 8d).

In the fourth step, probable sinkholes and karst areas were randomly chosen for field checking. Random samples were chosen by dividing the study area to equal cells and then randomly selecting different sinkholes and karst areas from some cells. To check susceptible sinkholes and karst features in the field, it was found that the selected areas are depressions filled with accumulation *red* sediments and sometimes including columnar structure of limestone rock which resist the dissolution process (Fig. 9). Field checking indicated that the enhanced techniques succeeded in mapping all areas of sediment accumulation (filled sinkholes and karst areas) in depressions that could be related to dissolution phenomena.

Causes and impact of karst and sinkholes

Different types of factors that could cause karst include the following: (1) Presence of soluble rocks: the geologic map of Egypt shows that a significant portion of Egypt covered by soluble rocks. (2) Presence of geologic structures: the chances of limestone dissolution increase with the presence of structures such as anticlines, joints, and faults. Faults, joints, and cracks are usually good pathways for water flow, and the formation of caves was confirmed by many investigations to be controlled by the fracture distribution. (3) Subsurface dissolution of evaporite rocks due to infiltration of surface waters (Youssef et al. 2011). Other areas could have the same phenomena in Egypt especially along the Red Sea coast due to the distribution of evaporite rocks. (4) Thickness of the overburden: the probability of the occurrence of sinkholes is high when the overburden of unconsolidated soil above the existing solution cavity is thin. Because the process of soil flow into the cavity is governed by a "piping" process, the speed of piping is a function of distance, which is represented by the thickness of the overburden. (5) Excessive groundwater pumping: karstification due to this factor may occur in areas characterized by excessive groundwater extraction from subsurface limestone aquifers. The top layers will subside or collapse due to dewatering of underneath cavities. (6) Irrigation and rainwater infiltration that cause karstification due to the wetting of the topsoil. This leads to the increase in the topsoil weight and decrease in its internal strength and cohesion. Moreover, infiltration of water through the top layers causes internal erosion processes and migration of sediments though underlying cavities and conduits. (7) Static and dynamic loads, such as external loads, man-made vibrations, and excavation, may trigger the collapse of unstable cavities (Tharp 2003; Pazuniak 1989); Gertje and Jeremias 1989; Iqbal 1995; Abdeltawab 2013).

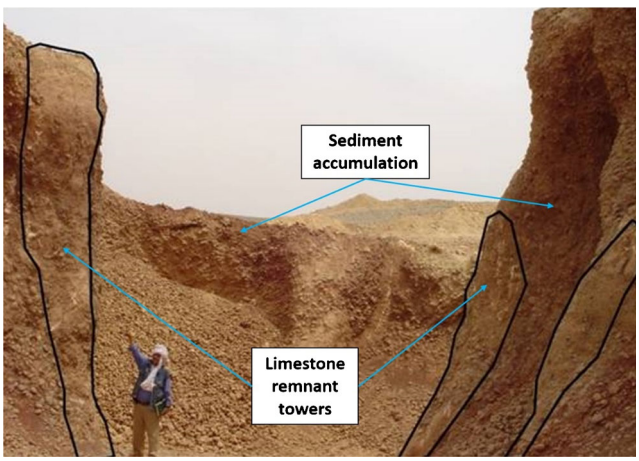

Fig. 9 Limestone towers remaining inside aggregate sediment

Karst can pose multiple hazards to urban areas and infrastructures, which need to be addressed through featured investigation methods (Gutiérrez et al. 2010; Parise 2010). These hazard types will have direct and indirect effect on different areas. The increasing human invasion of karst prone areas will enhance the hazard degree due to karst features. In many carbonate areas, solid limestone can present a high bearing capacity which is good for the foundation. However, the limestone is interspersed with open and sediment-filled voids as well as pinnacles at shallow depth that will complicate foundation design, subsurface homogeneity, integrity, and excavatability processes. These features underlying a proposed engineering project are unpredictable that will increase the challenges for the engineers in dealing with these features.

Conclusion and final considerations

A significant proportion of Egypt is underlain by soluble sediments, including Paleogene and Neogene limestone formations and evaporite in addition to Quaternary sabkhas. Karst hazard investigation in Egypt is a very cursorial work; however, this type of research is very rare and it is still beginning. The area around Sohag City provides an excellent location to investigate karst (sinkholes and cavities). The recent increase in sinkhole activities and their related hazards can be mainly contributed to human activities that enhance and/or trigger

subsidence phenomena. The majority of the karst features in the study area contribute to cavities formed in the past under humid conditions. Those cavities may have remained under equilibrium conditions for a long time, until some changes and/or alterations happened due to anthropogenic activities. The disequilibrium conditions can initiate or accelerate internal erosion and subsidence processes. Extensive field investigation was used to determine and classify different types of karst features in the study area. In addition, the integration of satellite remote sensing with the field data proved to be a successful method in identifying karst features. It was found that the karst features were distributed in many areas. Finally, application of remote sensing techniques and detailed field investigations proved to be useful and important tools to detect and map the prone areas that might be at risk for surface collapse.

For the final consideration, developing a systematic data collection and analysis to establish a database management system using geographic information system would be highly desirable in order to determine, assess, and manage different types of karst and/or sinkhole hazards. Application of geophysical techniques to the planning areas to understand the subsurface karst features. The karst database and geophysical works would help to determine the most karst-susceptible zones where detailed investigations and application of remediation/mitigation measures are the decision maker's priority.

References

Abdeltawab S (2013) Karst limestone geohazards in Egypt and Saudi Arabia. Int J Geoeng Case Histories 2:258–269. doi:10.4417/IJGCH-02-04-02

Alexander SC, Larson E, Bomberger C, Greenwaldt B, Alexander EC, Jr, Rahimi M (2013) Combining LiDAR, aerial photography, and PictometryH tools for karst features database management. In: Land L, Doctor DH Stephenson JB (eds) Proceedings of the Thirteenth Multidisciplinary Conference on Sinkholes and the Engineering and Environmental Impacts of Karst, National Cave and Karst Research Institute, Symposium 2, Carlsbad, pp 441–448

Amin AA, Bankher KA (1997) Karst hazard assessment of eastern Saudi Arabia. Nat Hazards 15:21–30. doi:10.1023/A:1007918623324

Boardman JW, Kruse FA (1994) Automated spectral analysis a geological example using AVIRIS data, northern Grapevine Mountains, Nevada. In: Proceeding 10th thematic conference on geologic remote sensing, San Antonio, Texas, 9–12 may, pp 407–418

Brook G, Embabi N, Edwards R, Cowart J, Dabous A (2002) Djara Cave in the western desert of Egypt: morphology and evidence of Quaternary climatic change. Cave Karst Sci 29(2):57–65

Carbonel D, Rodríguez-Tribaldos V, Gutiérrez F, Galve JP, Guerrero J, Zarroca M, Acosta E (2015) Investigating a damaging buried sinkhole cluster in an urban area (Zaragoza City, NE Spain) integrating multiple techniques: geomorphological surveys, DInSAR, DEMs, GPR, ERT, and trenching. Geomorphology 229:3–16. doi:10.1016/j.geomorph.2014.02.007

Crawford NC (1984) Sinkhole flooding associated with urban development upon karst terrain: bowling Green, Kentucky. In: Beck BF (ed) Proceedings of the first multidisciplinary conference on sinkholes. A.A. Balkema, Rotterdam, pp 283–292

Crosta A, Moore JMM (1989) Enhancement of landsat thematic mapper imagery for residual soil mapping in SW Minais Gerais State, Brazil: a prospecting case history in greenstone belt terrain. In: Proceedings of the seventh thematic conference on remote sensing for exploration Geology, Calgary, Alberta, Canada, 2–6 October, pp 1173–1187

De Carvalho O, Guimarães R, Montgomery D, Gillespie A, Trancoso Gomes R (2014) Karst depression detection using ASTER, ALOS/PRISM and SRTM-derived digital elevation models in the Bambuí Group. Brazil Remote Sens 6:330–351. doi: 10.3390/rs6010330

Dinger JS, Zourarakis DP, Currens JC (2007) Spectral enhancement and automated extraction of potential sinkhole features from NAIP imagery—initial investigations. J Environ Informatics 10(1):22–29. doi:10.3808/jei.200700096

El Naggar ZR (1970) On a proposed lithostratigraphic subdivision of the late cretaceous-early Paleocene succession in the Nile Valley. Egypt, UAR 7th Arab Petrol Congr, Kuwait 64(B-3):1–50

El-Ramly I (1997) El Mokattam City: karst problems. In: GÜNAY G, JOHNSON A (eds) Karst waters and environmental impacts. Proc. 1995 Symp. On karst waters and environmental problems, Antalya, Turkey, 10–20 sept. 1995. A.A. Balkema, Rotterdam, pp 85–92

El-Sayed M (1995) Duricrust and karst pinnacles in and around Farafra Oasis, western desert, Egypt. Sedimentology Egypt 3:27–38

Ford DC, Williams P (2007) Karst hydrogeology and geomorphology. John Wiley & Sons Ltd., Chichester, United Kingdom, p 562

Gao Y, Luo W, Jiang X, Lei M, Dai J (2013) Investigations of large scale sinkhole collapses, Laibin, Guangxi, China. In: Land L, Doctor DH, Stephenson JB (eds) Sinkholes and the engineering and environmental impacts of karst. National Cave and Karst Research Institute, pp 327–331

Gertje H, Jeremias EA (1989) Building construction over an erosive sinkhole site: a case study in Lancaster county Pennsylvania, USA. In: Proceedings of third multidisciplinary conference on sinkholes and the engineering and environmental impact of karst. Balkema, Rotterdam

Green AA, Berman M, Switzer P, Craig MD (1988) A transformation for ordering multispectral data in terms of image quality with implications for noise removal. IEEE Trans Geosci Remote Sens 26(1):65–74

Grosch JJ, Touma FT, Richards D (1987) Solution cavities in the limestone of eastern Saudi Arabia. In Multidisciplinary conference on sinkholes and the environmental impacts of karst 2:73–78

Guimarães RF, Carvalho Junior OA, Souza Martins EM, Carvalho APF, Gomes RAT (2005) Detection of karst depression by ASTER image in the Bambui Group. Brazil Proc SPIE 5983:328–339

Gunn J (ed) (2004) Encyclopedia of caves and karst science. Fitzroy Dearborn, New York, p 902

Gutiérrez F, Calaforra JM, Cardona F, Ortí F, Durán JJ, Garay P (2008) Geological and environmental implications of the evaporite karst in Spain. Environ Geol 53(5):951–965. doi:10.1007/s00254-007-0721-y

Gutiérrez F, Lucha P, Galve JP (2010) Reconstructing the geochronological evolution of large landslides by means of the trenching technique in the Yesa Reservoir (Spanish Pyrenees). Geomorphology 124(34):124–136. doi:10.1016/j.geomorph.2010.04.015

Gutiérrez F, Galve JP, Lucha P, Castañeda C, Bonachea J, Guerrero J (2011) Integrating geomorphological mapping, trenching, in SAR and GPR for the identification and characterization of sinkholes in the mantled evaporite karst of the Ebro Valley (NE Spain). Geomorphology 134:144–156

Gutiérrez F, Mozafari M, Carbonel D, Gómez R, Raeisi E (2014a) Leakage problems in dams built on evaporites. The case of La Loteta Dam (NE Spain), a reservoir in a large karstic depression

generated by interstratal salt dissolution. Eng Geol 185(5):139–154. doi:10.1016/j.enggeo.2014.12.009

Gutiérrez F, Parise M, De Waele J, Jourde H (2014b) A review on natural and human-induced geohazards and impacts in karst. Earth Sci Rev 138:61–88. doi:10.1016/j.earscirev.2014.08.002

Halliday W (2000) St. Anthony's cave, eastern desert of Egypt. In: 2000 Speleodigest, Natl. Spel. Soc., Huntsville, AL, USA. Reprinted from Speleograph, pp 302–332

Halliday W (2003) Caves and karsts of northeast Africa. Int J Speleol 32(1/4):19–32

Hume W (1925) Geology of Egypt. Government Press, Cairo, pp 1:91–1141 and Plates XLI and LI

Iqbal MA (1995) Engineering experience with limestone. In: Proc. 5th multidisciplinary conf. on sinkholes and the engineering and environmental impacts of karst. Balkema, Rotterdam, pp 463–468

Kareim MS (2001) Geomorphology of the east side of the River Nile. Sohag Bull Geog Soc Egypt 37:295–358

Khalil J, Hassan T (1997) Hydrogeological aspects of karstified aquifer and its environmental impacts in Eastern Desert, Egypt. In: GÜNAY G, JOHNSON A (eds) Karst waters and environmental impacts. Proc. 1995 Symp. On karst waters and environmental problems, Antalya, Turkey, 10–20 sept. 1995. A.A. Balkema, Rotterdam

Khalil J, El-Hossary M, Firky A (2002) Speleology of carbonate aquifer system in Siwa Oasis, Egypt. Proc. Symp. Middle-East Speleology 2001. Kaslik, Lebanon, pp 130–133

Laporte LF (1971) Paleozoic carbonate facies of the central Appalachian shelf. J Sediment Petrol 41(3):724–740

Mostafa HA (1979) Geology on the area northeast of Sohag. M.Sc. Thesis, Fac. Sci., Assiut Univ., Branch of Sohag, 259p.

Newton JG (1976) Early detection and correction of sinkhole problems in Alabama, with a preliminary evaluation of remote sensing applications: Alabama Highway Department, Bureau of Research and Development, Research Report no. HPR-76 Final Rpt., FHWA-RD-M-0305, 83 p

Parise M (2006) Geomorphology of the Canale di Pirro karst polje (Apulia, southern Italy). Zeitschrift für Geomorphologie NF 147: 143–158

Parise M (2010) Hazards in karst. In: Bonacci O (ed) Proceedings international inter-disciplinary scientific conference "sustainability of the karst environment. Dinaric karst and other karst regions": Plitvice Lakes (Croatia), 23-26 September 2009, IHP-UNESCO, Series on Groundwater no. 2, pp 155–162

Pazuniak BL (1989) Subsurface investigation response to sinkhole activity at an eastern Pennsylvania site. In Proceedings of the 3rd multidisciplinary conference on sinkholes. St. Petersburg Beach, FL 2: 263–269

Pielsticker KH (2002) Tropfsteine in der Ägyptischen Sahara (vorlaufiger Bericht). Mitt dt Höhlen- und Karstforsch 48(4):98–102

Ranjbar H, Honarmand M (2004) Integration and analysis of airborne geophysical and ETM+ data for exploration of porphyry type deposits in the central Iranian volcanic belt using fuzzy classification: Intl. J Remote Sens 25(21):4729–4741. doi:10.1080/01431160410001709011

Ruggieri R (2001) Speleologia d'Egitto. Speleologia. Soc Spel Italiana, Bologna 45:42–51

Said R (1960) Planktonic foraminifera from the Thebes Formation, Luxor, Egypt. Micropaleontology 16:227–286

Siart C, Bubenzer O, Eitel B (2009) Combining digital elevation data (SRTM/ASTER), high resolution satellite imagery (Quickbird) and GIS for geomorphological mapping: a multi-component case study on Mediterranean karst in Central Crete. Geomorphology 112:106–121

Singh A, Harrison A (1985) Standardized principal components. Int J Remote Sens 6(6):883–896. doi:10.1080/01431168508948511

Song KI, Cho GC, Chang SB (2012) Identification, remediation and analysis of karst sinkholes in the longest railroad tunnel in South Korea. Eng Geol 135-136:92–105. doi:10.1016/j.enggeo.2012.02.018

Tangestani MH, Moore F (2002) Porphyry copper alteration mapping at the Meiduk area. Iran: Intl J Remote Sens 23(22):4815–4825. doi:10.1080/01431160110115564

Tharp TM (2003) Cover- collapse sinkhole formation and soil plasticity. In: Sinkholes and engineering and environmental impacts of karst. ASCE, pp 110–123

Theilen-Willige B, Aït Malek H, Charif A, El Bchari F, Chaïbi M (2014) Remote sensing and GIS contribution to the investigation of karst landscapes in NW-Morocco. Geosciences 4(2):50–72. doi:10.3390/geosciences4020050

Waltham T, Bell F, Culshaw M (2005) Sinkholes and subsidence: karst and cavernous rock in engineering and construction. Springer, Berlin 382 p

Wanas HA, Soliman H, Pickford M, Ségalen L, Mein P (2009) Late Miocene karst system at Sheikh Abdallah, between Bahariya and Farafra, Western Desert, Egypt: implications for palaeoclimate and geomorphology. In Geologica acta 7:475–487

White WB (1988) Geomorphology and hydrology of karst terrains. Oxford University Press, Oxford, p 464

White WB (2002) Karst hydrology: recent developments and open questions. Eng Geol 65:85–105

White WB (2007) A brief history of karst hydrogeology: contributions of the NSS. Journal of Cave and Karst Studies 69:13–26

Wilson RCL (1975) Atlantic opening and Mesozoic continental margin basins of Iberia. Earth Planet Sci Lett 25(1):33–43

Youssef AM (2008a) An enhanced remote sensing procedure for material mapping in the western desert of Egypt: a tool for managing urban development. Nat Resour Res 17(4):215–226. doi:10.1007/s11053-008-9080-y

Youssef AM (2008b) Mapping the Pliocene clay deposits using remote sensing and its impact on the urbanization developments in Egypt: case study, east Sohag area. Geotech Geol Eng 26(5):579–591. doi:10.1007/s10706-008-9191-6

Youssef AM, Pradhan B, Sabtan AA, El-Harbi HM (2011) Coupling of remote sensing data aided with field investigations for geological hazards assessment in Jazan area, Kingdom of Saudi Arabia. Environ Earth Sci 65(1):119–130. doi:10.1007/s12665-011-1071-3

Youssef AM, Al-Qaluobi H, Zabramawi YA (2012) Integration of remote sensing and electrical resistivity methods in sinkhole investigation in Saudi Arabia. J Appl Geophys 87:28–39. doi:10.1016/j.jappgeo.2012.09.001

Youssef AM, Al-Harbi HM, Gutiérrez F, Zabramwi YA, Bulkhi AB, Zahrani SA, Bahamil AM, Zahrani AJ, Otaibi ZA, El-Haddad BA (2016) Natural and human-induced sinkhole hazards in Saudi Arabia: distribution, investigation, causes and impacts. Hydrogeol J 24(3):625644. doi:10.1007/s10040-015-1336-0